

THE VIRTUAL GAS TURBINE SYSTEM FOR ALLOY ASSESMENT

T. Yokokawa,¹ H. Saeki,² Y. Fukuyama,³ T. Yoshida,⁴ and H. Harada¹

¹ National Institute for Materials Science, High-Temperature Materials Group;
 1-2-1 Sengen, Tsukuba Science City, Ibaraki 305-0047, Japan

² Toshiba Corporation, Power & Industrial Systems R&D Center;
 2-4 Suehiro-cho, Tsurumi-ku, Yokohama 230-0045, Japan

³ Japan Aerospace Exploration Agency, Aeronautical Environment Technology Center;
 7-44-1 Jindaiji-higashi, Chofu, Tokyo 182-8522, Japan

⁴ Japan Aerospace Exploration Agency, Aeronautical Environment Technology Center
 (Now in Tokyo University of Agriculture and Technology, Department of Mechanical Systems Engineering);
 2-24-16 Nakacho, Koganei, Tokyo, 184-8588, JAPAN

Key words: Virtual turbine, Alloy design program, Gas turbine design program, Nickel-base superalloy

Abstract

In the "High Temperature Materials 21" (HTM21) project, we developed a virtual gas turbine (VT) system as a combination of an alloy design program and a gas turbine design program. The VT is a simplified automatic gas turbine simulation program that can be used on personal computers. The VT performs simplified aerodynamic, cooling, and structural analysis calculations based on preset design parameters, which were tuned for a medium-size 1300°C-class land-base gas turbine. By using the VT, we estimate the plant performance (thermal efficiency, CO₂ emission rate, etc.) as well as the life of the components, such as the creep rupture life of blades, for any new superalloys with arbitrary alloy compositions. In this study, the following alloys were evaluated in the VT with the turbine inlet gas temperature (TIT) up to 1700°C : Rene-N5 and TMS-82+ ; (second-generation SC superalloys), and TMS-138 and TMS-138++ ; (fourth- and fifth-generation SC superalloys containing Ru).

Introduction

The improvement of the thermal efficiency of a gas turbine (GT) can be achieved by an increase of the turbine inlet gas temperature (TIT). However, in using GT blades or vanes made of conventional materials, the increase of coolant consumption with the increase of the TIT reduces the efficiency of GTs. Therefore, the development of advanced high-temperature materials, such as new-generation Ni-base single-crystal (SC) superalloys or possible alternative materials, is expected to realize a higher temperature GT with less coolant consumption. Some material design programs have been published as tools for the development of new materials. For example, a series of alloys with excellent mechanical properties has been developed using the alloy design program (ADP) for Ni-base superalloys[1,2]. On the other hand, various simulation techniques, such as computational fluid dynamics (CFD) using supercomputers, have also been developed to assist in the design of turbine systems. Unfortunately, material scientists and GT designers have had limited opportunities to evaluate newly developed materials for real GTs. To improve this situation, a gas turbine simulation program, called a virtual gas

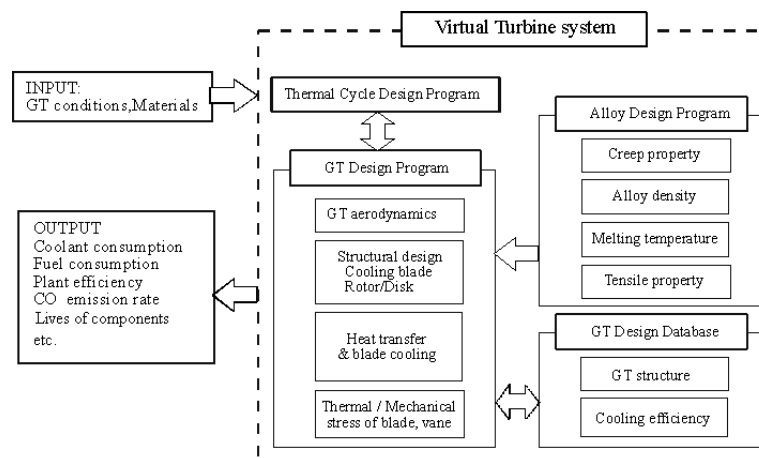


Fig.1. Schematic diagram of the virtual gas turbine (VT) system.

turbine system (VT)[3], was developed by integrating the ADP and the gas turbine design program (GTDP). In this paper, the principal features of the present VT and its application for materials design are described.

Outline of the Virtual Gas Turbine System

The VT is mainly composed of an alloy design program (ADP) and a gas turbine design program (GTDP) with a thermal cycle design program (TCDP), as shown in **Figure 1**.

The inputs for the VT are the GT power output level, GT inlet temperature (TIT), and vane and blade materials. The ADP is used for the prediction of the structural and mechanical properties of materials for vanes and blades under turbine-operating conditions. The GTDP designs a gas turbine under the given conditions by consulting other inter-connected design programs and databases. The most important function of GTDP is to estimate the temperatures and stress levels of vanes and blades under given coolant flow-rate conditions. These estimated values are also used for the life estimation of the vanes and blades. The TCDP determines the rotational speed of the GT rotor, the GT pressure ratio, and the fuel flow rates to realize a given TIT and send the calculated results back to the GTDP.

In the present VT system constructed on Excel[®] work sheets, whole design processes are controlled by the macro function and repeated until two convergence criteria, that are the coolant flow rate and the turbine exhaust pressure, are satisfied.

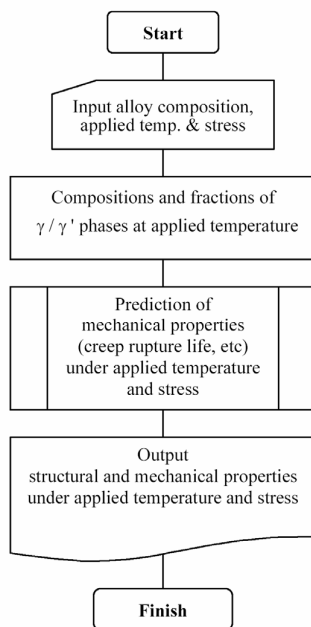


Fig. 2. Schematic calculation flow chart of our alloy design program (ADP).

Alloy Design Program

In the present VT system, the ADP is available for Ni-base SC superalloys with arbitrary compositions, including those with platinum group metal (PGM) elements, under various temperatures and stresses. This ADP is currently used for alloy development of multi-component Ni-base superalloys[4,5] at the National Institute for Materials Science.

Figure 2 shows the flow chart of the ADP. When the alloy composition, applied temperature, and stress are input, the structural properties, such as the chemical compositions of the γ and γ' phases, volume fraction of the γ' phase, and lattice misfit between the γ and γ' phases, are calculated from the given alloy composition and temperature. Then, the mechanical properties, such as the creep rupture life, are predicted by regression equations that take not only the alloy composition into account but also the structural parameters, such as the γ / γ' lattice misfit and the volume fraction of the γ' phase.

In order to calculate the compositions of γ and γ' phases in equilibrium, the partitioning coefficient of alloying elements, including PGM elements, was derived by the regression analysis of 44 pairs of γ and γ' compositions, which were measured using an Electron Probe X-ray microanalyzer (EPMA). For example, **Figure 3** shows the partitioning behaviors of alloying elements in the Ru-bearing Ni-base superalloys containing 5wt% Re. It is clear that the partitioning behavior of the alloying elements is not changed by the Ru addition [6]. **Table 1** shows excellent agreement between the calculated and measured compositions of γ and γ' phases in equilibrium for various alloys with the results obtained from the EPMA.

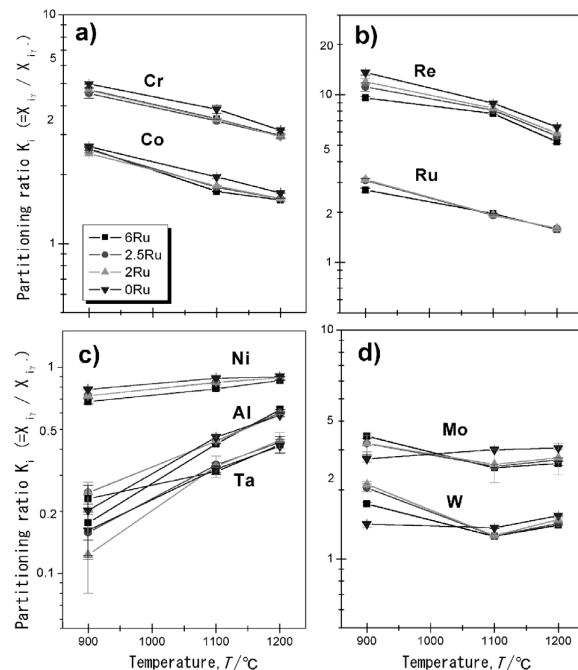


Fig. 3. Partitioning behaviors of alloying elements in various Ru bearing Ni-base superalloys containing 5wt% Re.

Table 1. Comparison between calculated and observed chemical compositions of γ and γ' phases for several superalloys (at%).

Alloy	Temp.		Phase	Co	Cr	Mo	W	Al	Ti	Nb	Ta	Hf	Re	PGM's
Rene N5	1120	Calc.	γ'	5.0	6.1	0.9	0.7	12.7	4.6	2.7	-	-	-	-
			γ	9.4	20.7	2.8	1.3	4.7	2.2	1.9	-	-	-	-
		Obs.	γ'	4.6	4.0	0.5	0.6	13.2	6.2	2.6	-	-	-	-
			γ	8.4	17.0	2.3	1.1	6.8	2.5	1.6	-	-	-	-
TMS-1	1240	Calc.	γ'	6.4	3.1	-	4.2	17.0	-	-	2.5	-	-	-
			γ	9.4	9.4	-	6.9	8.9	-	-	1.3	-	-	-
		Obs.	γ'	5.8	2.8	-	3.3	17.2	-	-	2.9	-	-	-
			γ	8.5	7.5	-	6.2	11.4	-	-	1.6	-	-	-
TMS-75	1100	Calc.	γ'	9.6	1.5	0.6	1.9	17.4	-	-	2.9	0.06	0.5	-
			γ	15.9	5.9	2.0	2.1	9.6	-	-	1.1	0.01	3.0	-
		Obs.	γ'	10.0	1.8	0.7	1.6	16.9	-	-	2.7	0.03	0.4	-
			γ	18.2	6.4	1.9	2.2	8.9	-	-	1.0	N.A	3.1	-
TMS-75 +Ir	1100	Calc.	γ'	9.3	1.4	0.6	1.9	17.5	-	-	2.9	0.06	0.5	Ir1.0
			γ	15.6	5.7	1.9	2.1	9.7	-	-	1.1	0.01	2.9	1.0
		Obs.	γ'	9.5	1.8	0.7	1.6	16.9	-	-	2.8	0.02	0.4	0.9
			γ	16.8	6.0	1.8	2.2	9.1	-	-	1.1	N.A	3.0	0.9
TMS-75 +Ru	1100	Calc.	γ'	9.2	1.4	0.6	1.9	17.1	-	-	2.9	0.06	0.5	Ru0.7
			γ	15.5	5.7	1.9	2.1	9.5	-	-	1.1	0.01	2.8	1.2
		Obs.	γ'	9.3	1.7	0.7	1.7	16.3	-	-	2.9	0.02	0.4	0.7
			γ	16.4	5.7	1.7	2.1	8.9	-	-	1.1	-	2.8	1.2
TMS-75 +Pt	1100	Calc.	γ'	9.2	1.4	0.6	1.9	17.6	-	-	3.0	0.06	0.5	Pt1.3
			γ	15.5	5.6	1.9	2.1	9.7	-	-	1.1	0.01	2.8	0.6
		Obs.	γ'	9.3	1.7	0.7	1.6	17.2	-	-	2.8	0.04	0.4	1.1
			γ	17.1	5.6	1.8	2.2	8.9	-	-	1.0	N.A	3.0	0.5

Table 2. Structural parameters and mechanical properties which can be predicted by our alloy design program (ADP)

Abbreviation	Items	Unit	Condition
(WT%)	Alloy composition	wt%	—
(AT%)	Alloy composition	at%	—
GP	Composition of γ /phase	at%	Applied temp.
G	Composition of γ' phase	at%	Applied temp.
FractionGp	Volume fraction of γ /phase	-	Applied temp.
LatGp	Lattice parameter of γ /phase	Å	Applied temp.
LatG	Lattice parameter of γ' phase	Å	Applied temp.
LatMisfit	Lattice misfit	%	Applied temp.
Sl	Solubility limit	—	1173K
Density	Density	g/cm ³	R.T
Elong.	Elongation	%	Applied temp.
RA	Reduction of area	%	Applied temp.
SC life	Creep rupture life for SC superalloys	h	Applied temp. & stress

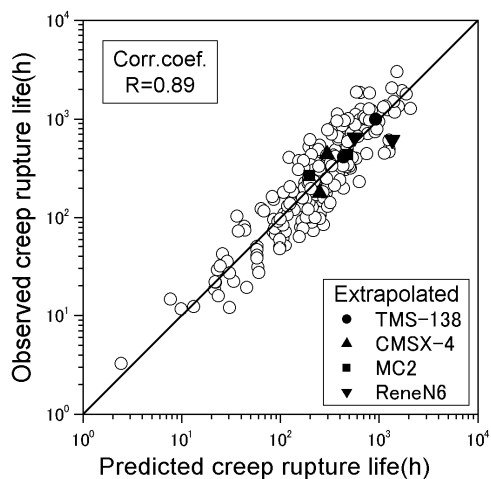


Fig. 4. Relationship between calculated and observed creep rupture life.

For the prediction of the mechanical properties of SC superalloys, for example, the creep rupture life, an equation was developed by the regression analysis of creep test data for 57 different SC alloys under the conditions of 750-1150°C and 98-735MPa. This equation expresses the creep rupture life as a function of the γ' composition, γ' volume fraction, γ/γ' lattice misfit, applied temperature, and stress. **Figure 4** shows excellent agreement between the calculated and measured creep rupture lives. In this figure, solid marks show the results for the alloys, CMSX-4 [7], MC2 [8], ReneN6 [9], and TMS-138 [10], which were not used to derive the regression equation for the creep rupture life.

Table 2 shows all structural parameters and mechanical properties that can be predicted in this ADP.

Thermal Cycle Design Program

The TCDP controls the VT system by monitoring the overall plant heat and mass balance. The thermal power plant that can be designed by the present TCDP is a simple-cycle GT system or a GT/ST combined cycle system. **Figure 5** shows the thermal cycle schematics of a combined cycle power plant. The ambient air is compressed through the compressor (from 1 to 5) and then introduced into the combustor (from 5 to 7). The high-temperature and high-pressure gas flow which is generated by the combustor is then led to the turbine. The hot gas is expanded to the atmospheric pressure while generating power (rotating the generator). Turbine exhaust gas that is still hot is led to the heat-recovery steam generator (HRSG) to generate steam (from 7 to 10). The generated steam expands in the steam turbine. The present VT treats the working gas as a mixture of five component gases (N_2 , O_2 , H_2O , CO_2 , and Ar), and the thermal properties are computed at all points by referring to the temperature, pressure, and gas concentrations. The primary and intended function of the VT is to clarify the influence of the development and introduction of a new material, such as a Ni-base SC superalloy, to virtual high-temperature GTs. From the viewpoint of the greenhouse effect, the influences may be measured by the thermal efficiency of a power plant and the CO_2 emission rate. In addition, these values are computed in this TCDP. The TCDP can burn liquid fuels as well as gaseous fuels. Therefore, the influence of fuel is also simulated. The optimization of the GT pressure ratio is also incorporated in the TCDP, and the user can select the modes from the maximum power output and maximum thermal efficiency.

Gas Turbine Design Program

The real design process of a gas turbine requires an extremely large number of calculations. It was most important in the development of the VT to reduce the calculation time while retaining the required accuracy. The GTDP must complete the aerodynamic, cooling, and structural calculations on a personal computer in a relatively short time. However, to obtain a clear difference for the vane-row and blade-row from stage to stage, the aerodynamic design is based on velocity triangle calculations, taking the cooling injection effects into account. The points of cooling and structural design are the assessment of the vane bending stress, the blade centrifugal stress, and the bulk temperature for the evaluation of the creep life and of the metal surface temperature for the evaluation of the oxidation or corrosion life. The influence of thermal barrier coating (TBC) is also considered in the GTDP. The GT coolant flow rate must be determined so that all design limitations coming from considering the blade life are clarified. However, this process requires much computational time, since the coolant flow rate must be given for all the vanes and blades for each stage and the changes in coolant flow rates influence the thermal cycle heat balance and mass balance. To solve this highly complicated system, the VT has the outer convergence loop to balance the dependent variables (coolant flow rates, coolant temperature, and gas turbine stage load) by an iterative procedure. To minimize complexity to the user, most of the design parameters, such as the rotor disk and blade proportions, internal cooling structure, external film-cooling hole distributions for vanes and blades, and combustor outlet temperature distribution, are contained in a database.

Cooling Characteristic Databases

The cooling characteristics, namely, the databases for the cooling efficiency versus coolant flow rate against the blade-cooling configurations and the film-cooling effectiveness, are also very important for the correct estimation of the temperature of the blade metal. These databases have been developed based on experimental data and the results of advanced large-scale computational fluid dynamics (CFD) [11,12].

For example, the average and minimum cooling effectiveness for the first-stage vane and blade are given below:

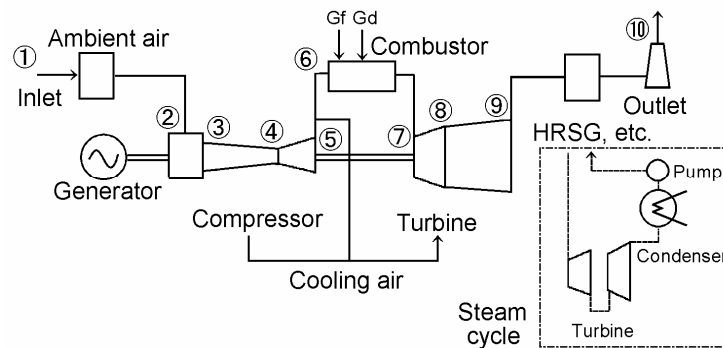


Fig. 5. Diagram of the combined-cycle power plant in the virtual gas turbine system

<Vane>

$$\text{average: } \eta_{av} = 0.714 \{ 1 - \exp(-0.47(Gc/Gg)) \} \quad (1)$$

$$\text{minimum: } \eta_{min} = 0.660 \{ 1 - \exp(-0.47(Gc/Gg)) \} \quad (2)$$

<Blade>

$$\text{average: } \eta_{av} = 0.608 \{ 1 - \exp(-0.43(Gc/Gg)) \} \quad (3)$$

$$\text{minimum: } \eta_{min} = 0.507 \{ 1 - \exp(-0.43(Gc/Gg)) \} \quad (4)$$

where Gg is the main gas flow rate and Gc is the cooling gas flow rate.

Figure 6 shows the agreement of the cooling effectiveness between experimental data and the equations given above. These equations can only predict a one-dimensional feature of the sophisticated distribution of the temperature of the blade metal. To take the two-dimensional surface temperature distribution effects into account, 3D-CFD with a film-cooling injection was performed, and the results will be integrated in the next-generation VT. Figure 7 indicates the vane surface temperature and streamline considering the film-cooling injection. The computed main flow gas temperature (Fig. 7(a)), film-cooling effectiveness, and surface heat-transfer coefficient (Fig. 7(b)) give the vane and blade surface thermal boundary conditions for the structural analysis. By using the calculated two-dimensional distributions, the characteristic curves of the mean and minimum cooling effectiveness were derived for root, 10%, 30%, 50%, 70%, 90%, and tip cross-sections. Figure 8 indicates the sectional mean cooling-effectiveness characteristic versus the coolant flow-rate ratio for the different vane height cross-sections. By applying the newly developed cooling-characteristic curves noted above, the estimations of creep and oxidation will be more accurate.

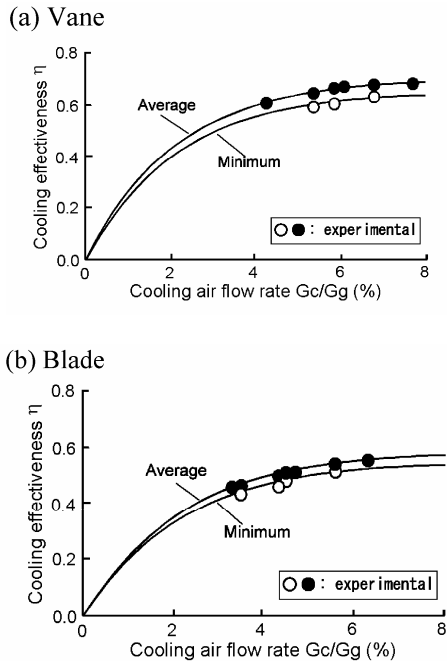
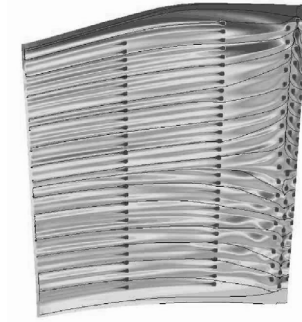


Fig. 6. Agreement of the cooling effectiveness between experimental data and prediction equation formulas.

(a)



(b)

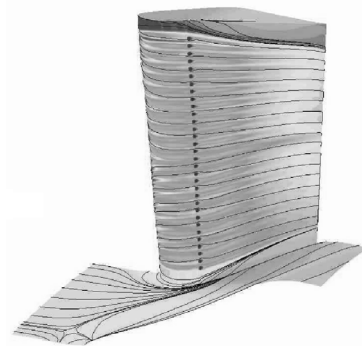


Fig. 7. Example of CFD calculation for the three dimensional film cooled gas turbine vane.

(a). Temperature distribution of vane surface.
(b). Streamline of vane surface.

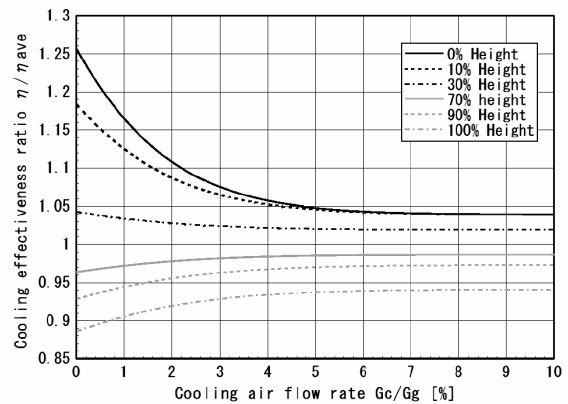


Fig. 8. One-dimensional cooling effectiveness curves for different vane height cross sections.

Application Example of VT

Figure 9 shows the Input/Output worksheet of the VT system. The main inputs and outputs are listed below.

- Inputs: Gas turbine output power level (e.g., 180MW)
 Turbine inlet gas temperature (e.g., 1500°C)
 Blade/vane materials (e.g., TMS-82+)
 Thickness of thermal barrier coating layer (e.g., 0.1mm)
- Outputs: Turbine gas path profiles
 Coolant airflow rates
 Thermal efficiency of GT and C/C plant
 CO2 emission rate
 Performances of blades and vanes (e.g., creep strength)

The VT was used to evaluate conventional and developed SC superalloys, such as Rene-N5 [13], TMS-82+ [14], TMS-138 [10], and TMS-138++ [5], and the turbine performance in terms of the thermal efficiency of the 180MW C/C power plant, specific power per ambient airflow rate, and specific CO₂ emission rate per output power. The temperature capabilities under a 137MPa - 1000h creep rupture life are 1025°C for Rene-N5, 1075°C for TMS-82+, 1083°C for TMS-138, and 1100°C for TMS-138++.

In Figures 10 and 11, it is clear that, if Rene-N5 is replaced with TMS-82+ as the blade material, the thermal efficiency of the C/C power plant will increase by about 1%, and the specific power will increase by about 10%, even if the TIT is the same; this is because the coolant airflow rate is decreased and the

principal airflow rate is increased. The thermal efficiency of a C/C power plant can reach 55% (HHV) by increasing the TIT to 1600°C provided that the coolant airflow rate is increased up to the limitation of 30%. If TMS-138 or TMS-138++ is used as the blade material, the TIT can be increased to more than 1600°C. For example, the thermal efficiency can reach 56.5% (HHV) with a TIT of 1700°C if TMS-138++ is used, and the specific CO₂ emission rate is decreased from 175(kg/s)/kW to 165 (kg/s)/kW, as shown in Figure 12. Further improvements in the thermal efficiency are expected with a more sophisticated cooling system, such as steam cooling, which will be applied to an actual 1700°C-class turbine system.

Further improvements of the VT system are in progress; for example, an equation that fits the creep curve is produced as follows:

$$\varepsilon = I \times (A_1 + S_2 + S_3) \quad (5)$$

$$I = \exp(-\exp((t - \mu) / c_1))$$

$$S_i = A_i \exp((t - \lambda) / c_i)$$

where, ε is the creep strain, t is the time in hours, I and A_1 are correspond to the primary creep stage, S_2 and S_3 are correspond to the secondary and tertiary creep regions, μ , λ , and c_i are the constants, respectively.

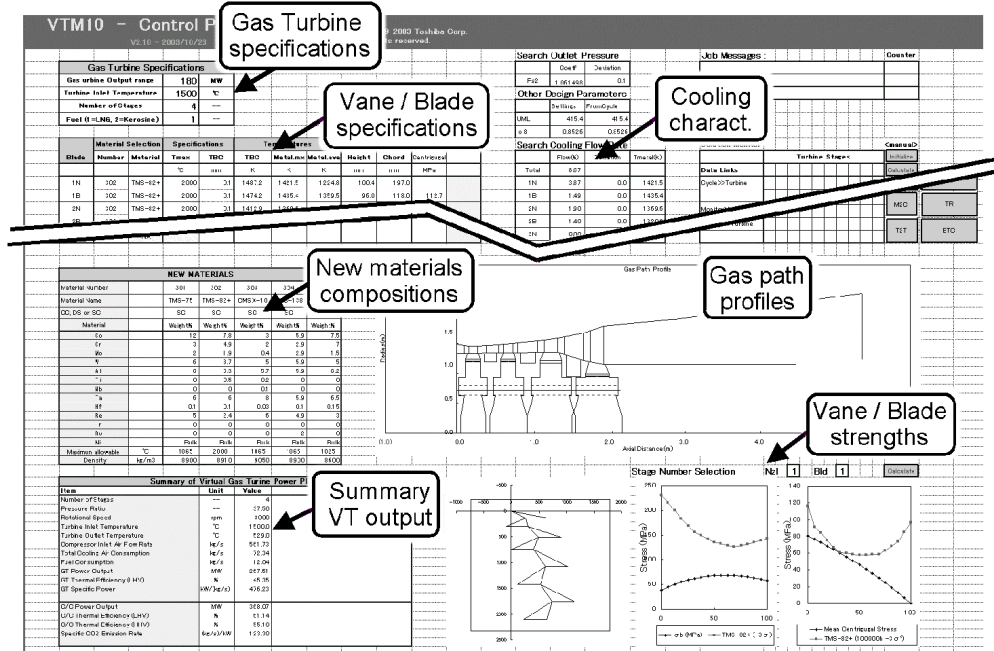


Fig. 9 Input/Output worksheet of the VT system.

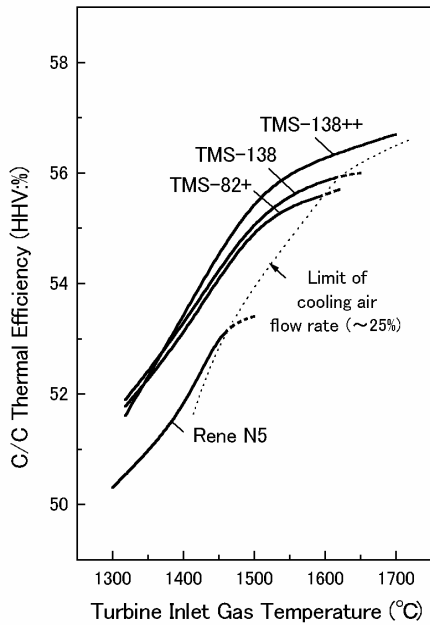


Fig. 10. Relationship between the thermal efficiency and the inlet gas temperatures.

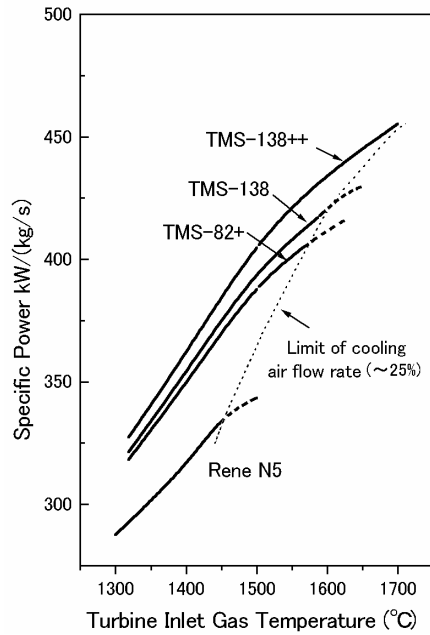


Fig. 11. Relationship between the specific power and the inlet gas temperatures.

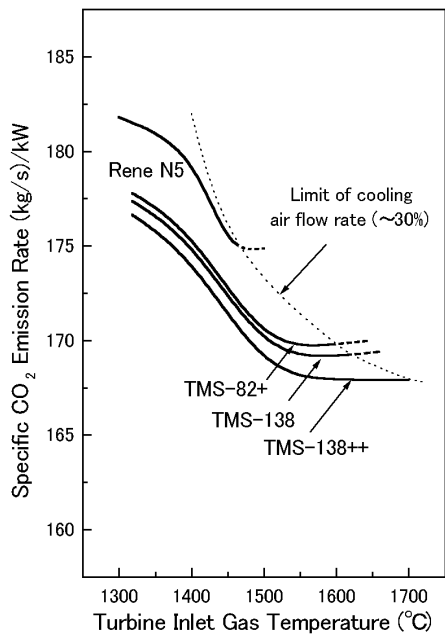


Fig. 12. Relationship between specific CO₂ emission rate and the inlet gas temperatures.

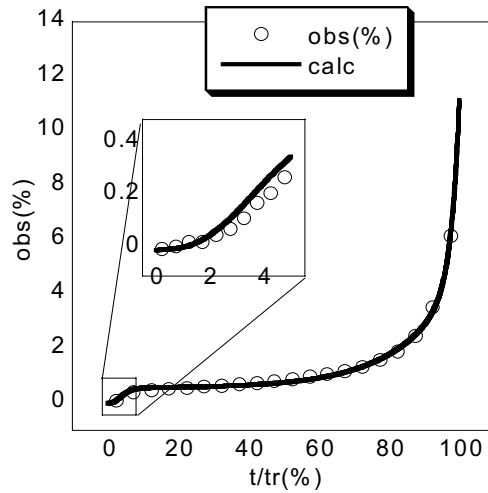


Fig. 13. Agreement between the fitted and observed creep curves of the TMS-75 alloy under 1100°C-137MPa.

Figure 13 shows excellent agreement between the fitted and the observed creep curves of a TMS-75[5] alloy under 1100°C-137MPa. The research aims to determine the relationship among the constants, the alloy composition, the temperature, and the stress through regression analysis. Thus, the blade can be evaluated in the VT system by more practical specifications, e.g., 1% local creep deformation, or total creep deformation of the component which correspond to their of a gas turbine system employed industrially.

Conclusions

A virtual gas turbine system (VT) was developed by a combination of an alloy design program for Ni-base superalloys (ADP) and a gas turbine design program (GTDP).

By using VT, the plant performance, such as the thermal efficiency and CO₂ emission rate, can be estimated, as well as the lives of components for newly developed Ni-base single-crystal superalloys with an arbitrary alloy composition. As a result of the estimation of the performance for 180MW combined-cycle power plant, the thermal efficiency of a 1700°C-class C/C system that uses a TMS-138++ alloy can reach 56.5% (HHV), and 165 (kg/s)/kW specific CO₂ emission rate. Further improvements in the thermal efficiency are expected with a more sophisticated cooling system, such as steam cooling, which will be applied to an actual 1700°C-class turbine system.

Acknowledgements

The VT study has been conducted in the High Temperature Materials 21 Project based at NIMS, Japan, and is now being exploited for the development of virtual aero-engine. The authors are also grateful to Ms. T. Odaka and Mr. H. Izuno for the creep data analysis.

References

1. H. Harada, et al., "Phase Calculation and Its Use in Alloy Design Program for Nickel-base Superalloys," *Superalloys 1988*, TMS, 733 (1988).
2. H. Harada, et al., "Calculation of Gamma-Prime/Gamma Equilibrium in Multi-Component Nickel-base Superalloys," *Proc. Conference on High-Temperature Materials for Power Engineering 1990*, European Commission, 1319 (1990).
3. H. Saeki, et al., "Development of a Gas turbine Design Program Coupled with an Alloy Design program – A Virtual Turbine," *International Gas Turbine Congress*, Tokyo, TS-122 (2003).
4. T. Kobayashi, et al., "Design of High Rhenium Containing Single Crystal Superalloys with Balanced Intermediate and High Temperature Creep Strength," *Proc. 4th International Charles Parsons Turbine Conference*, The Institute of Materials, 766 (1997).
5. Y. Koizumi, et al., "Development of New-Generation Ni-base Single Crystal Superalloys" to be presented at the Superalloys 2004 conference.
6. T. Yokokawa, et al., "Partitioning Behavior of Platinum Group Metals on the γ . and γ' Phases of Ni-base Superalloys at High Temperatures.," *Scripta Mater.* 49, 1041 (2003).
7. K. Harris, et al., "Development of the Rhenium Containing Superalloys CMSX-4 and CM 186 LC for Single Crystal Blade and Directionally Solidified Vane Applications in Advanced Turbine Engines," *Superalloys 1992*, 297 (1992).
8. P. Caron and T. Khan, "Development of a New Nickel-Base Single Crystal Turbine Blade Alloy for Very High Temperatures," *Proc. First European Conference, EUROMAT 89*, FRG, 22 (1989).
9. W. Walston, et al., "Rene N6: Third Generation Single Crystal Superalloy," *Superalloys 1996*, TMS, 27 (1996).
10. J.X. Zhang, et al., "Interfacial Dislocation Networks Strengthening a Fourth-Generation Single-Crystal TMS-138 Superalloy," *Metall. Mater.*, 33A, 3741 (2002).
11. J. Ishii, I. Sato and Y. Fukuyama, "Development and Testing of 15MW Class Heavy Duty Gas turbine," *Proc. CIMAC Congress*, 479 (1998).
12. T. Yoshida, et al., "Virtual Turbine: Itss State of the Art and Advenced Works in the Project," *Proc. High Temperature Materials 2001*, NIMS (2001).
13. C.S. Wukusick and L. Buchakjian, "Nickel-Base Superalloys," *U.K. Patent Appl.* GB2235697, (1991).
14. T. Hino, et al., "Development of a new single crystal superalloy for industrial gas turbines," *Superalloys 2000*, TMS, 729 (2000).